Research Journal of Applied Sciences, Engineering and Technology 6(4): 687-690, 2013
DOI:10.19026/rjaset.6.4181
ISSN: 2040-7459; e-ISSN: 2040-7467

Submitted: September 13, 2012 Accepted: October 19, 2012 Published: June 20, 2013

**Research Article**

# Fully-developed Turbulent Pipe Flow Using a Zero-Equation Model

Khalid Alammar
Mechanical Engineering Department, King Saud University, Riyadh 11421, Kingdom of Saudi Arabia,
P.O. Box 800, Tel.:+ 96614676650; Fax: + 96614676652

**Abstract:** Aim of this study is to evaluate a zero-equation turbulence model. A fully-developed turbulent pipe flow was simulated. Uncertainty was approximated through grid-independence and model validation. Results for mean axial velocity, $u^+$ and Reynolds stress had maximum error of 5%, while results for the friction factor had negligible error. The mean axial velocity was shown to increase and extend farther in the outer layer with increasing Reynolds number, up to $10^6$. There was no effect of Reynolds number on $u^+$ below wall distance, $Y^+$, of 100. Similar to the friction velocity, peak of the Reynolds stress was shown to increase and extend farther in the outer layer with increasing Reynolds number. There was no effect of Reynolds number on Reynolds stress below wall distance of 20. The new turbulence model is equally applicable to developing and external flows using the same constant. For wall-bounded flows, the constant is a function of wall roughness.

**Keywords:** Reynolds stress, skin friction, turbulence modeling

## INTRODUCTION

The problem of turbulence dates back to the days of Claude-Louis Navier and George Gabriel Stokes, as well as others in the early nineteenth century. Searching for its solution, it was a source of great despair for many notably great scientists, including Werner Heisenberg, Horace Lamb and many others. The complete description of turbulence remains one of the unsolved problems in modern physics. A great deal of early work on turbulence can be found, for example, in Hinze (1975).

Recently, Direct Numerical Simulation (DNS) has emerged as an indispensible tool to tackle turbulence directly, albeit at relatively low Reynolds numbers. Several DNS studies on turbulent pipe flow have been performed recently, including Eggels *et al*. (1993), Loulou *et al*. (1997) and Wu and Moin (2008). The latter has carried out DNS on a turbulent pipe flow at Reynolds number of 44,000, which is the largest among the three studies. Mean velocity, Reynolds stresses and turbulent intensities are presented and discussed, along with visualization of flow structure. Good agreement was attained with the Princeton Superpipe data on mean flow statistics and Lawn (1971) data on turbulence intensities. Large Eddy Simulation (LES) is another tool that somewhat bridges between DNS and Reynolds-averaged Navier-Stokes (RANS) methods. In LES, large turbulent structures in the flow field are resolved, while the effect of Sub-Grid Scales (SGS) are modeled. LES investigation, for example, has been carried out by Rudman and Blackburn (1999) using LES on a turbulent pipe flow at Reynolds number of 38,000. Mean velocity and Reynolds stresses are presented and discussed, along with visualization of flow structure. Results were reported to compare favorably with measurements.

While DNS and LES are fairly accurate for modeling turbulent flows, they remain limited to relatively low-range Reynolds numbers. This drawback explains the wide-spread of turbulence modeling in industrial applications where the use of DNS techniques remains formidable. Turbulence modeling includes eddy viscosity models which utilize the Boussinesq hypothesis, Hinze (1975), for relating the Reynolds stresses to the average flow filed. In turn, the eddy viscosity is determined by using any of a variety of techniques, including the zero-equation, one-equation and two-equation models, most notably the k-□ model. While such models vary in complexity, they share several shortcomings, including isotropy of the eddy viscosity and the lack of generality in wall treatment. Such shortcomings lead to poor results in separated flows and other non-equilibrium turbulent boundary layers, Yamamoto *et al*. (2008).

A second-order turbulence model, which also falls under RANS methods, is the Reynolds stress model. While the model relaxes the isotropic assumption, it remains more complicated and costly due to the need for solving six additional transport equations along with many unknown terms. For more on the subject of turbulence modeling, the reader is referred to, for example, Launder and Spalding (1972).

In this study, the accuracy of a zero-equation turbulence model is assessed. Unlike typical eddy-viscosity models, the proposed model does not require

the solution of additional transport equations and requires one constant which is strictly a function of wall roughness. Moreover, the model does not require a wall function because the momentum equation is integrated throughout the flow field. The new model is equally applicable to external flows. For simplicity, steady, axisymmetric and fully-developed pipe flow is considered.

**Theory:** Starting with the incompressible Navier-Stokes equations in Cartesian index notation and with Reynolds decomposition, averaging and following Boussinesq hypothesis, we have:

$$\frac{\partial(\overline{u}_i)}{\partial x_i} = 0 \tag{1}$$

$$\rho\left[\frac{\partial(\overline{u}_i)}{\partial t} + (\overline{u}_j)\frac{\partial(\overline{u}_i)}{\partial x_j}\right] + \frac{\partial(\overline{p})}{\partial x_i} - \frac{\partial}{\partial x_j}\mu\left(\frac{\partial \overline{u}_i}{\partial x_j} + \frac{\partial \overline{u}_j}{\partial x_i}\right) = \frac{\partial}{\partial x_j}\mu_t\left(\frac{\partial \overline{u}_i}{\partial x_j} + \frac{\partial \overline{u}_j}{\partial x_i}\right) \tag{2}$$

For simplicity, the normal stresses (except for the thermodynamic pressure) and body forces are neglected. $\mu_t = C\mathrm{Re}_t\,\mu$ is the eddy viscosity (Alammar, 2008). C is a non-dimensional function of the wall roughness. For a smooth wall, it is a constant. For isotropic roughness, it is a different constant. $\mathrm{Re}_t = |\overline{u}_i|\rho d/\mu$ and d is the distance to the nearest wall. C, therefore, takes the value of that location at the wall. When Eq. (2) is normalized, the shear stresses result in the following:

$$\frac{\partial}{\partial x_j}\left[\mathrm{Re}^{-1} + C\frac{|\overline{u}_i|d}{UD}\right]\left(\frac{\partial \overline{u}_i}{\partial x_j} + \frac{\partial \overline{u}_j}{\partial x_i}\right) \tag{3}$$

The second term in the brackets is a non-dimensional number attributed to turbulence. Clearly, this term dominates at high Reynolds numbers. In absence of walls, one plausible length scale would be the mean free path. This would give rise to second-order effects that would be negligible in presence of walls.

Using cylindrical coordinates, Fig. 1 and assuming steady, axisymmetric and fully-developed pipe flow, we have (after integration once with respect to r):

$$(\mu + \mu_t)\frac{du}{dr} = \frac{r}{2}\frac{dP}{dx} \tag{4}$$

The constant of integration vanishes due to symmetry condition at the center point. The eddy viscosity is given by:

$$\mu_t = c\rho u d \tag{5}$$

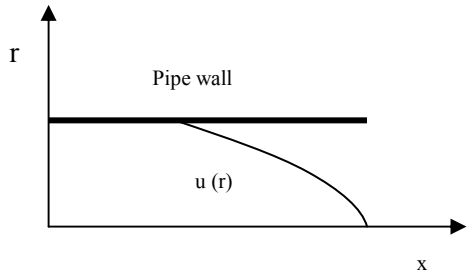


Fig. 1: Schematic of the pipe with fully-developed flow

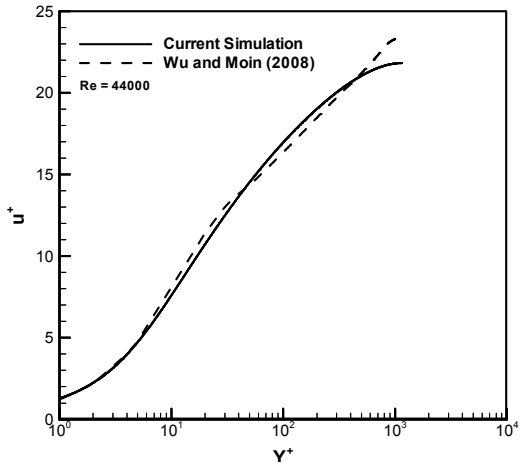


Fig. 2: Mean axial velocity profiles for Re = 44,000

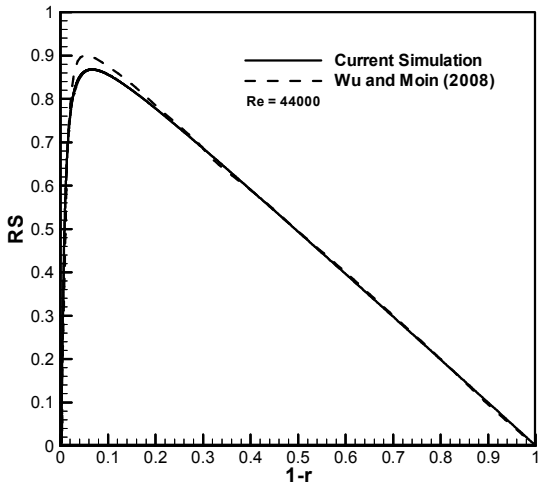


Fig. 3: Reynolds stress profiles for Re = 44,000

where c = 0.016, d is the distance from the wall and the pressure gradient is constant.

**Numerical procedure and uncertainty analysis:** There are mainly two sources of uncertainty in Computational Fluid Dynamics (CFD), namely modeling and numerical, Stern *et al*. (1999). Modeling uncertainty can be approximated through theoretical or

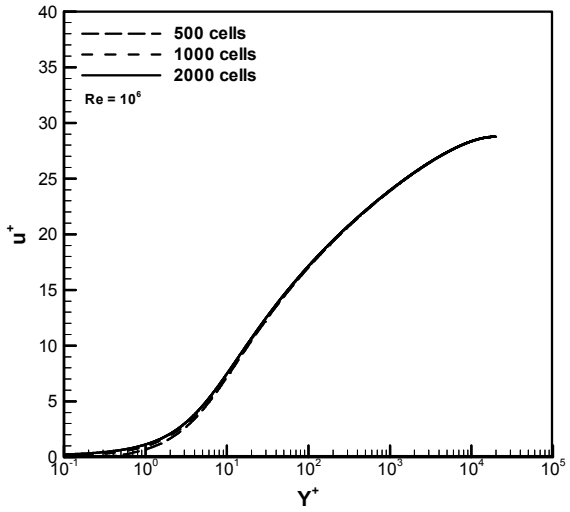


Fig. 4: Mean axial velocity profiles for Re = $10^6$

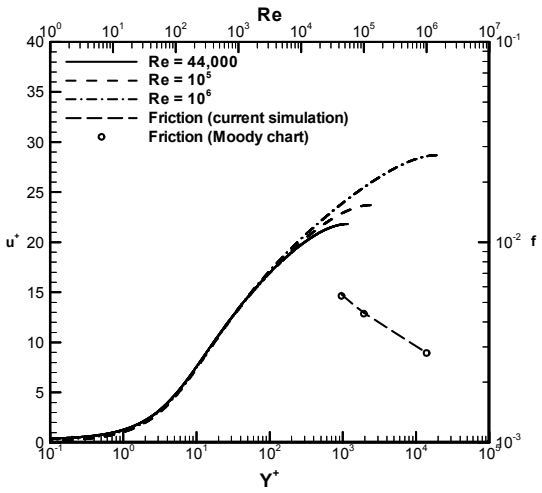


Fig. 5: Mean axial velocity profiles and friction factor for various Reynolds numbers

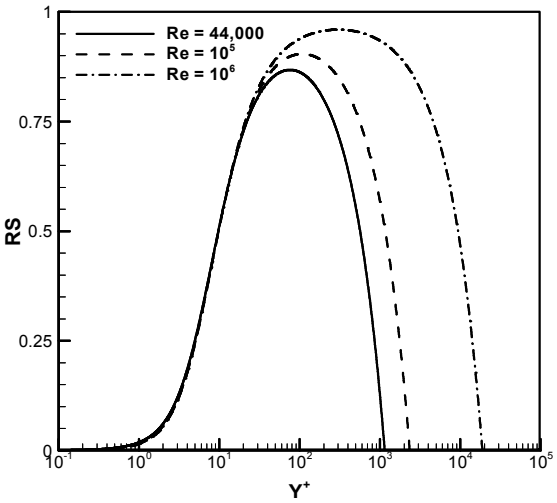


Fig. 6: Reynolds stress profiles for various Reynolds numbers

experimental validation while numerical uncertainty can be approximated through grid independence. Numerical uncertainty has two main sources, namely truncation and round-off errors. Higher order schemes have less truncation error. In explicit schemes, round-off error increases with increasing iterations and is reduced by increasing significant digits (machine precision).

Equation (4) was solved using the Euler second-order algorithm with the no-slip boundary condition. The fully-developed mean axial velocity is depicted in Fig. 2 for Reynolds number of 44,000, along with DNS results of Wu and Moin (2008). The discrepancy is <±5%. Such discrepancy could be attributed, in part, to transitional effects in the buffer layer. At the center of the pipe, the discrepancy could be attributed to the enforcement of symmetry condition. The Reynolds stress is shown in Fig. 3 for Reynolds number of 44,000. Again, good agreement is attained between the current simulation and the DNS results, with the discrepancy restricted within the buffer layer and is <±5%.

A grid-independence test is depicted in Fig. 4 for three different, non-uniform cell sizes, namely 500, 1000 and 2000. The error in $u^+$ is mostly in the laminar sub-layer and is shown to be negligible with 2000 cells for Reynolds number of $10^6$. Hence, we can conclude that the overall uncertainty in the current numerical results is ±5%.

## RESULTS AND DISCUSSION

The fully-developed mean axial velocity is depicted in Fig. 5 for various Reynolds numbers up to $10^6$. The mean velocity is shown to increase and extend farther in the outer layer with increasing Reynolds number. This is in agreement with published measurements, e.g., Laufer (1954). There is no effect of Reynolds number on the mean velocity below wall distance of 100. The friction factor is also shown in Fig. 5 and compared with data from the Moody chart, Moody (1944). The agreement is excellent.

The Reynolds stress is depicted in Fig. 6 for various Reynolds numbers up to $10^6$. Similar to the mean velocity, peak of the Reynolds stress is shown to increase and extend farther in the outer layer with increasing Reynolds number. There is no effect of Reynolds number on the profiles below wall distance of 20. This is different from the case of $u^+$ where the change was negligible below wall distance of 100.

## CONCLUSION

Using a zero-equation turbulence model, fully-developed turbulent pipe flow was simulated. Results for the mean axial velocity and Reynolds stress had maximum error of 5%, while results for the friction

factor had negligible error. Mean axial velocity was shown to increase and extend farther in the outer layer with increasing Reynolds number. There was no effect of Reynolds number on $u^+$ below wall distance of 100. Similar to the mean axial velocity, peak of the Reynolds stress was shown to increase and extend farther in the outer layer with increasing Reynolds number. There was no effect of Reynolds number on the profiles below wall distance of 20. The new turbulence model is equally applicable to developing and external flows using the same constant for smooth walls. For wall-bounded flows, the constant is a function of wall roughness. This study was conducted in the year 2012 at the college of Engineering, King Saud University, Riyadh main campus.

## NOMENCLATURE

C = A non-dimensional function of wall roughness
D = Pipe diameter, m
d = Normal distance from the wall, m
f = Friction factor = $\tau_w/0.5\rho U^2$
Re = Reynolds number = $U\rho D/\mu$
$Re_t$ = Non-dimensional parameter = $|\overline{u_i}|\rho d/\mu$
RS = Reynolds stress = $-\rho\overline{u'v'}/\tau_w$, Pa
U = Area-average velocity, m/s
$U_*$ = Friction velocity = $\sqrt{\tau_w/\rho}$, m/s
$\overline{u_i}$ = Mean velocity component, m/s
u = Mean axial velocity, m/s
$u^+$ = Normalized mean axial velocity = $u/U_*$
$x_i$ = Cartesian coordinate, m
$y^+$ = Non-dimensional wall distance = $rU_*\rho/\mu$
r = Radial distance, m
$\mu$ = Fluid dynamic viscosity, Pa s
$\rho$ = Fluid density, kg/m$^3$
$\tau_w$ = Wall shear stress, Pa

## REFERENCES


Alammar, K., 2008. Turbulence: A new zero-equation model. 7th International Conference on Advancements in Fluid Mechanics, Wessex Institute of Technology, New Forest, UK, May 21-23.

Eggels, J., F. Unger, M. Weiss, J. Westerweel, R. Adrian, R. Friedrich and F. Nieuwstadt, 1993. Fully developed turbulent pipe flow: A comparison between direct numerical simulation and experiment. J. Fluid Mech., 268: 175-209.

Hinze, J.O., 1975. Turbulence. McGraw-Hill Publishing Co., New York.

Laufer, J., 1954. The structure of turbulence in fully developed pipe flow. U.S. National Advisory Committee for Aeronautics (NACA), Technical Report 1174.

Launder, B.E. and D.B. Spalding, 1972. Mathematical Models of Turbulence. Academic Press Inc., London.

Lawn, C.J., 1971. The determination of the rate of dissipation in turbulent pipe flow. J. Fluid Mech., 48: 477-505.

Loulou, P., R. Moser, N. Mansour and B. Cantwell, 1997. Direct simulation of incompressible pipe flow using a B-Spline spectral method. Technical Report: TM-110436, NASA-Ames Research Center, pp: 168.

Moody, L.F., 1944. Friction factors for pipe flow. Transactions of the A.S.M.E, pp: 671-684.

Rudman, M. and H. Blackburn, 1999. Large eddy simulation of turbulent pipe flow. Second International Conference on CFD in the Minerals and Process Industry, CSIRO, Melbourne, Australia, Dec. 6-8.

Stern, F., R. Wilson, H. Coleman and E. Paterson, 1999. Verification and Validation of CFD Simulation. Iowa Institute of Hydraulic Research IIHR 407, College of Engineering, University of Iowa, Iowa City, IA, USA, 3.

Wu, X. and P. Moin, 2008. A direct numerical simulation study on the mean velocity characteristics in turbulent pipe flow. J. Fluid Mech., 608: 81-112.

Yamamoto, Y., T. Kunugi, S. Satake and S. Smolentsev, 2008. DNS and k-ε model simulation of MHD turbulent channel flows with heat transfer. Fusion Eng. Des., 83(7-9): 1309-1312.